
Received: 19 August 2024, Accepted: 14 November 2024

Edited by: C. Brito

Licence: Creative Commons Attribution 4.0

DOI: <https://doi.org/10.4279/PIP.160003>



ISSN 1852-4249

Critical behavior of rumor propagation on random networks of cliques

Lucas A Sobehart,¹ Damián H Zanette^{1,2*}

We disclose a critical phenomenon induced by structural properties of the contact pattern in a stylized model of rumor propagation over a population of agents. The contact pattern is given by a random network of cliques, formed by fully interconnected groups of nodes of identical size with randomly distributed connections between groups. As demonstrated numerically using finite-size scaling analysis, the process exhibits a critical transition between a regime where the rumor remains confined to a negligible part of the population and a regime where it attains a finite portion of the system. We determine the critical point and the critical exponent of the transition for different clique sizes. The phenomenon is analogous to that observed for the same kind of process in Watts-Strogatz small-world networks, and is likely due to the combination of large clustering and short mean geodesic distances that also characterizes random networks of cliques.

I Introduction

The behavior of dynamical processes in systems of interacting agents can strongly depend on the structure of their interaction patterns. The interplay between underlying geometrical and/or topological properties and emerging collective dynamics in such systems has been a subject of primary interest since the inception of network science [1]. In the vast corpus of research dealing with this question, some of the earliest work focused on the effects of network structure on percolation and epidemics spreading [2–4], as reviewed in Ref. 5. More recently, much attention has been devoted to the cases of synchronization processes [6–8], neuronal dynamics [9–11], and ecological and biochemical

systems [12–14], among others. In Refs. 15 and 16, it was shown that a stylized process of rumor propagation evolving on a Watts-Strogatz small-world network [17] exhibits a critical transition as the topological disorder in the network increases. Concretely, the rumor remains confined to a negligible part of the network with low disorder and reaches a finite portion if the disorder overcomes a certain critical threshold.

In a recent contribution [18], we have introduced a class of networks consisting of ensembles of cliques –namely, fully interconnected, relatively small groups of nodes– sparsely connected to each other by randomly distributed links. These random networks of cliques (RNoCs) aim to capture a widespread topological feature of real-life interaction networks, specifically, the segregation of agents in compact groups with relatively sparse connections between groups. This kind of architecture is found in a variety of socioeconomic complexes, where division into communities plays crucial roles [19–23], and is also observed in other natural [24–26] and artificial systems [27]. In RNoCs, large interconnectivity between nodes inside cliques

* damian.zanette@ib.edu.ar

¹ Centro Atómico Bariloche and Instituto Balseiro, Comisión Nacional de Energía Atómica and Universidad Nacional de Cuyo, Av. Ezequiel Bustillo 9500, 8400 San Carlos de Bariloche, Argentina.

² Consejo Nacional de Investigaciones Científicas y Técnicas, Argentina.

ensures a high degree of clustering, while random inter-clique connections determine short average geodesic distances, typically of the order of the logarithm of the network size [18]. The combination of large clustering and short distances is diagnostic of the small-world nature of RNoCs, much as in the classic Watts-Strogatz model [17, 28].

In this paper, we disclose a critical phenomenon in a model of rumor propagation on RNoCs, qualitatively similar to that observed in Watts-Strogatz networks, as quoted above [15, 16]. The transition is induced by the density of inter-clique connections, which is one of the basic structural properties of the underlying network. Even when the number of inter-clique links is enough to connect most of the network –i.e. when a giant component is already present– their density must exceed a certain critical value to allow the rumor to reach a substantial portion of the system. In the next section, we introduce the subclass of RNoCs in which we study this phenomenon and quantitatively characterize their structural features. In Section III, we introduce the dynamical rules that define the model of rumor propagation and present results obtained from numerical simulations showing the existence of two well-differentiated regimes in the process, depending on the density of inter-clique links. In Section IV, we perform the finite-size scaling analysis that demonstrates the critical nature of the transition between the two regimes, obtaining estimations for the critical point and exponents. Finally, Section V is devoted to a summary of results and to our concluding remarks.

II Random networks of cliques (RNoCs)

A random network of cliques (RNoC) is constructed by first taking a collection of Q cliques. In the simplest version, all cliques are equal in size, each containing m nodes ($m \geq 3$), so that the total network size is $N = mQ$. Then, inter-clique links are established randomly by connecting pairs of nodes in different cliques, with the condition that at most one inter-clique link reaches each node. If γ is the probability that a node is reached by an inter-clique link, the expected total number of these links is $\gamma N/2$. The total number of links, including both intra- and inter-clique links, is, on average, $(m - 1 + \gamma)N/2$.

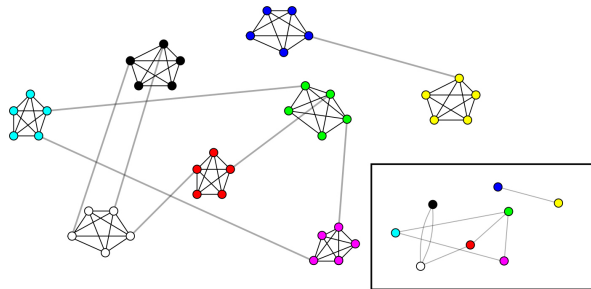


Figure 1: Main panel: A random network of cliques formed by $Q = 8$ cliques of size $m = 5$, and 8 inter-clique links ($\gamma = 0.4$). The inset shows the surrogate network, where each clique has been replaced by a single node, keeping the inter-clique links as connections between nodes.

The condition that each node is connected to at most one inter-clique link facilitates the analytical computation of the RNoC structural properties [18], quoted below.

As an illustration, the main panel of Fig. 1 shows a small RNoC, with $Q = 8$, $m = 5$, and 8 inter-clique links, corresponding to $\gamma = 0.4$. The network in the inset is a surrogate graph where each clique of the RNoC has been replaced by a single node, preserving the inter-clique links between nodes. By construction, the surrogate graph is an Erdős-Rényi random network, to which a variety of exact theoretical results are applicable. Note that, as shown in the figure, the surrogate graph can have multiple connections between pairs of nodes. This is not an inconvenience by itself, as the theory of random networks applies to such a situation [1]. In any case, the probability of multiple connections between cliques is of order Q^{-1} , and therefore decreases as larger networks are considered.

The degree distributions [29] of the RNoC and its surrogate graph –respectively, g_k and g_k^S – are

$$g_k = \frac{\gamma k}{m} \delta_{k,m} + \frac{(1-\gamma)(k+1)}{m} \delta_{k+1,m}, \quad (1)$$

where $\delta_{i,j}$ is Kronecker delta, and

$$g_k^S = \binom{m}{k} \gamma^k (1-\gamma)^{m-k}, \quad (2)$$

for $0 \leq k \leq m$. Since each clique is internally fully connected, the overall connectivity of the RNoC is determined by that of the surrogate graph and, consequently, by the degree distribution g_k^S . Applying

the formalism of generating functions [30], we find that, in the limit $Q \rightarrow \infty$, a giant component exists if $\gamma > \gamma_0$, with

$$\gamma_0 = \frac{1}{m-1}. \quad (3)$$

For $\gamma > \gamma_0$, the fraction of the network in the giant component is given by

$$G = 1 - u^{m/(m-1)}, \quad (4)$$

where u is the nontrivial ($u \neq 1$) solution to $u = [1 + \gamma(u-1)]^{m-1}$.

In the limit of large Q , clustering [29] can be exactly quantified for RNoCs. The mean and the global clustering coefficients are, respectively,

$$C_M = 1 - \frac{2\gamma}{m}, \quad C_G = \frac{m-2}{m-2+2\gamma}. \quad (5)$$

Note that C_M and C_G are functionally independent quantities, with $C_M \geq C_G$ for fixed m . Both are decreasing functions of γ , starting at $C_M = C_G = 1$ for $\gamma = 0$ and dropping to $C_M = C_G = 1 - 2/m$ for $\gamma = 1$. Moreover, they approach each other in the limit of large m . Generally, they have rather large values, with a minimum of $C_M = C_G = 1/3$ at $m = 3$ and $\gamma = 1$. This high level of clustering, even for large densities of the randomly distributed inter-clique links, is a direct consequence of the full connectivity inside each clique.

The geodesic distance between pairs of nodes [29] in the RNoC, given by the number of links along the shortest path joining the two nodes, is also controlled by the surrogate graph. In fact, among the $N(N-1)/2$ pairs of nodes all over the network, the number of pairs where the two nodes belong to the same clique is of order Q while the number of pairs with nodes in different cliques is of order Q^2 . The latter, thus, dominate the average geodesic distance L in large networks. In turn, if the nodes belong to two different cliques, their geodesic distance is essentially twice the geodesic distance between the surrogate nodes of the two cliques. Indeed, for each link along a path in the surrogate graph, one additional link is required in the original RNoC to travel between any two nodes inside each clique. Consequently, since in an Erdős-Rényi random network the average geodesic distance is of the order of the logarithm of the network size, in the RNoC we have $L \sim \log Q$ as well. The same relation to Q holds for

the network diameter, given by the longest geodesic distance between pairs of nodes.

As commented in the Introduction, the combination of an average geodesic distance that grows as the logarithm of the network size, and large clustering coefficients which, as in Eq. (5), are independent of size when the network is large, is a clue to the small-world nature of RNoCs. These are the same structural properties that identify, characteristically, the Watts-Strogatz construction [17].

Two other structural properties that can be given analytical values for RNoCs are assortativity [29],

$$r = \frac{2m^2(3-2\gamma)(m-1+\gamma) + m\gamma(1-\gamma)^2}{m\gamma(m-1)(1-\gamma)}, \quad (6)$$

and modularity [29],

$$q \approx \frac{m(m-1)}{m(m-1+\gamma)}. \quad (7)$$

For the latter, the result is an approximation for large Q , assuming that the optimal modular partition of the network is given by the division into cliques [18].

In the next section, we study a contact process –mimicking the propagation of a rumor– in a population where the contact pattern between agents is an RNoC of the type defined above. In particular, we focus on the effectiveness of propagation, measured by the fraction of the system reached by the rumor, as a function of the density of inter-clique links γ and for various values of the clique size m .

III Rumor propagation on RNoCs: dynamical rules and numerical results

In the last two decades, a wide variety of rumor propagation models on networks have been advanced, motivating much subsequent work (for a recent review, see Ref. 31). All these variants are based on some long-established proposals [32–34], and bear close relation to well-known epidemiological models, especially, of the SIR type [35]. At any given time during the evolution, each node in the network is in one of three states which, by analogy with SIR epidemiological models, are called susceptible (S), infected (I), and recovered (R). Susceptible individuals have not heard the rumor yet, infected individuals have heard the rumor and are

willing to transmit it, and recovered individuals have heard the rumor but have lost interest and do not transmit it.

The process runs as follows: At each time step, an infected node and one of its neighbors –say, i and j , respectively– are chosen at random. If j is susceptible, it becomes infected by rumor transmission. In this case, since communication between the two nodes has already occurred, the pair (i, j) will never be chosen again in the subsequent evolution. If, on the other hand, j , having already heard the rumor, is either infected or recovered, i then becomes recovered due to loss of interest. Moreover, if i has been fully disconnected from the network due to previous interactions, it also becomes recovered. In all cases, the time step is assigned a duration N_I^{-1} , where N_I is the number of infected nodes before the interaction occurs. Thus, on average, each infected node undergoes one interaction event per time unit. Initially, all nodes are susceptible except for a randomly chosen one, which is infected. The process of rumor propagation ends when no infected nodes remain in the population, and every node is either susceptible or recovered. Note that the main difference between these dynamical rules of rumor propagation and those of standard SIR models resides in the fact that the transition between the infected and the recovered states requires an interaction between agents, while in epidemiological dynamics it occurs spontaneously.

A suitable measure of the effectiveness of rumor propagation on the RNoC is given by the fraction of recovered nodes, n_R , at the end of the evolution. It gives the proportion of the population that has heard the rumor at some point during the process. If propagation is limited to an isolated clique, not connected to other cliques, it can be easily seen that, necessarily, $n_R = 1$ for cliques of size $m = 3$ or 4. As m grows, the average of n_R over realizations of the process decreases, approaching an asymptotic value of about 0.79 for large m .

For comparison with these values of n_R , we mention that, in a fully connected network, the fraction of the population reached by the rumor is $n_R \approx 0.8$ [34]. Since, on average, each infected node transmits the rumor just one time along the whole process, the same figure for n_R is expected in Erdős-Rényi random networks with a well-developed giant component, i. e. with a moderately large mean number of neighbors per node [1].

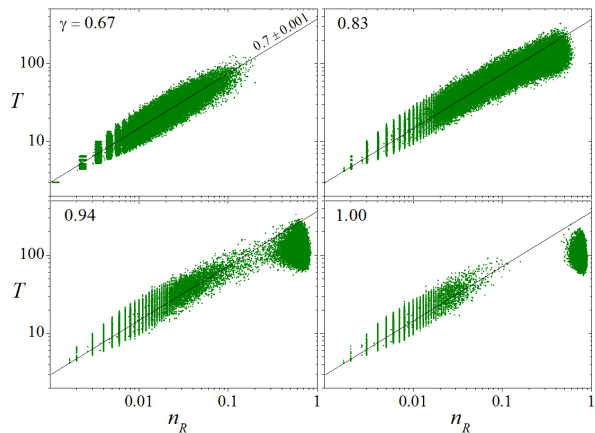


Figure 2: Total evolution time T vs. final fraction of recovered nodes n_R obtained in 10^5 realizations of the rumor propagation model on the giant component of RNoCs with $Q = 10^3$, for clique size $m = 3$ and four values of the density of inter-clique connections γ , in log-log scales. The straight lines have a slope of 0.7.

To assess the properties of rumor propagation on RNoCs, we ran series of 10^5 realizations of the process over the giant (largest) component of networks formed by $Q = 10^3$ cliques, for various values of the size of individual cliques, m , and of the density of inter-clique connections, γ (see Section II). Given m , the values of γ are chosen well above $\gamma_0 = (m - 1)^{-1}$, in the region where the giant component comprises a large part of the network [cf. Eq. (3)]. In each realization, we measured the fraction $n_R = N_R/N_G$, with N_R being the number of recovered nodes at the end of the evolution and N_G the number of nodes in the giant component.

In Fig. 2, we plot the pairs (n_R, T) in the case of $m = 3$, for four values of γ . For $\gamma = 0.67$, results are confined to small values of n_R , mostly below $n_R = 0.1$, and times which rarely reach above $T = 100$. On average, there is a well-defined algebraic relation between the two quantities, $T \propto n_R^p$ with $p = 0.700(1)$, as illustrated by the straight line. As γ grows and the network becomes better connected, the distribution of points on the plane (n_R, T) becomes progressively bimodal, giving rise to two separate clouds. Increasingly few points remain in the original cloud, which preserves the algebraic relation between n_R and T . Most realizations, in fact, now belong to the new cloud, with substantially higher values of n_R and maximal val-

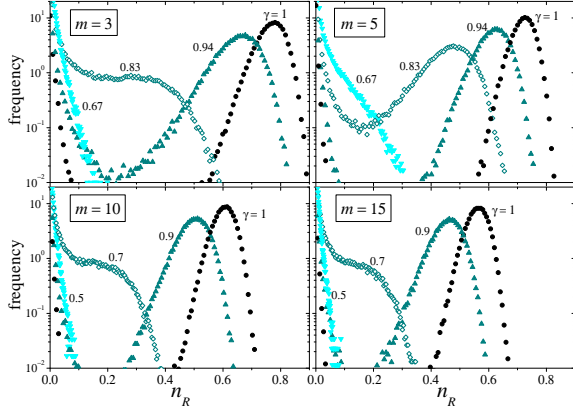


Figure 3: Histograms of the final fraction of recovered nodes n_R for four values of the clique size m , and four values of the density of inter-clique connections γ for each m . Data obtained from 10^5 realizations as in Fig. 2 for each parameter set.

ues of T situated between 200 and 300. For $\gamma \lesssim 1$, hence, realizations are divided into two categories. In some of them, the rumor reaches a relatively small portion of the network, typically below 10%, and remains confined to a few cliques. More frequently, however, the rumor is eventually heard by more than 60% of the population. Interestingly, while the two clouds are detached from each other in n_R , they have a non-negligible overlap in T , around $T = 100$.

The transition between unimodal and bimodal distributions in the final number of recovered nodes as the network connectivity grows is also observed for other clique sizes. Figure 3 shows histograms of n_R for four values of m , and four values of γ for each m , as obtained from a series of 10^5 realizations for each parameter set. The progressive development of a maximum at large values of n_R as γ increases is apparent in all cases. Note that the appearance of the maximum occurs at lower values of γ for larger clique sizes m . This effect can be ascribed to the fact that the larger the value of m , the larger the inter-clique connectivity for a given value of γ –i.e. the larger the connectivity in the surrogate network; cf. Eq. (2). At the same time, as discussed above for isolated cliques, the fraction of nodes within each clique that is expected to be reached by the rumor decreases with m . A consequence of the combination of these two opposite

trends is that the average value of n_R over realizations, which we denote as $\langle n_R \rangle$, can depend non-monotonically on m for intermediate values of γ . This is illustrated in Fig. 4, which shows $\langle n_R \rangle$ as a function of γ for the same values of m as in Fig. 3. For $\gamma = 0.9$, for instance, $\langle n_R \rangle$ first increases and then decreases with m .

In any case, the behavior of $\langle n_R \rangle$ with γ always shows a passage between a regime of low values for small γ , corresponding to the unimodal distributions of Fig. 3, to a rather fast growth for large γ , determined by the appearance of the large- n_R peak in the distributions. This behavior may be pointing to the occurrence of a critical transition as γ grows, much as observed in Watts-Strogatz small-world networks for increasing disorder [15, 16]. In the next section, indeed, we show that numerical evidence supports the existence of a critical point, and we present an estimation of the critical parameters associated with the transition.

IV Critical transition in rumor propagation: finite-size scaling

To assess whether a critical transition occurs in the mean final fraction of recovered nodes $\langle n_R \rangle$ as a function of the density of inter-clique links γ , we apply finite-size scaling analysis [36]. This requires studying the behavior of $\langle n_R \rangle$ versus γ as the sys-

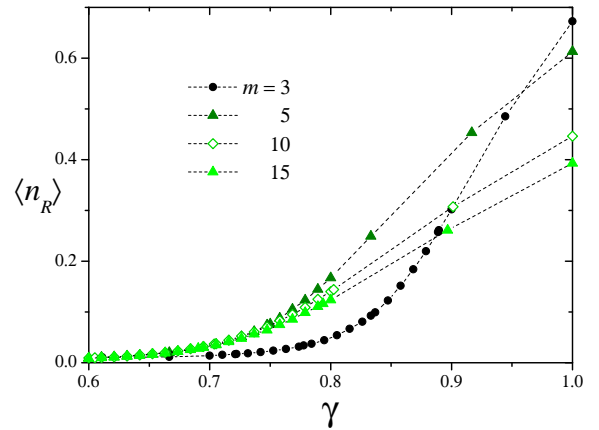


Figure 4: Mean fraction of final recovered nodes $\langle n_R \rangle$ as a function of the density of inter-clique connections γ , for four values of the clique size, averaged over 10^5 realizations as in Fig. 2.

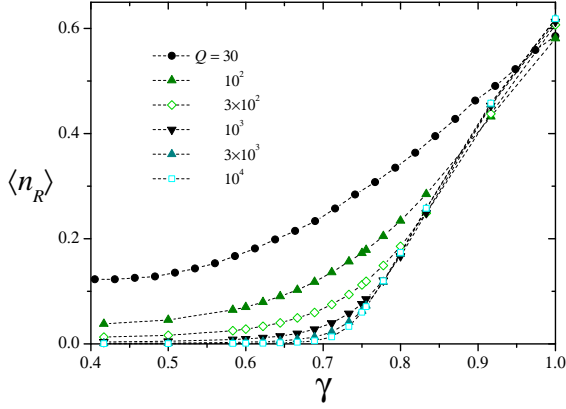


Figure 5: Mean final fraction of recovered nodes $\langle n_R \rangle$ as a function of the density of inter-clique links γ , for six values of the number of cliques Q , in the case of cliques of size $m = 5$.

tem size is varied. We illustrate the procedure with the case $m = 5$. Figure 5 shows results for six values of the number of cliques Q .

Following the methodology of finite-size scaling analysis, we assume that near the putative critical value of γ , $\gamma \approx \gamma_c$, and for sufficiently large networks, $Q \gg 1$, the order parameter $\langle n_R \rangle$ satisfies

$$Q^{\alpha\beta} \langle n_R \rangle = F(Q^\beta |\gamma - \gamma_c|), \quad (8)$$

with a yet-unknown function F and suitable values of the exponents α and β . This ansatz implies that, for $Q \rightarrow \infty$, $\langle n_R \rangle$ behaves as

$$\langle n_R \rangle \propto |\gamma - \gamma_c|^\alpha \quad (9)$$

near the transition. Thus, α is the main critical exponent, controlling the behavior of $\langle n_R \rangle$ in the vicinity of the critical point γ_c . For $\gamma = \gamma_c$, Eq. (8) predicts that $\langle n_R \rangle$ decays as a power of the network size:

$$\langle n_R \rangle = F(0)Q^{-\alpha\beta}. \quad (10)$$

The exponent β can be seen to control the divergence of the correlation length near the critical point [36]. Equation (10) makes it possible to estimate γ_c by studying how $\langle n_R \rangle$ behaves with Q as γ is varied.

Figure 6 shows numerical results for $\langle n_R \rangle$ as a function of Q for several values of γ . Two different behaviors are apparent. As Q grows, $\langle n_R \rangle$ tends to

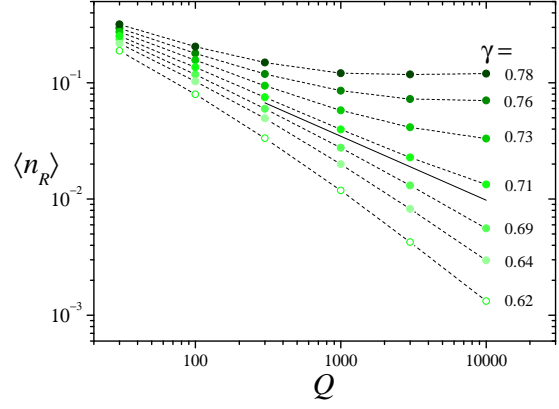


Figure 6: Mean final fraction of recovered nodes $\langle n_R \rangle$ as a function of the number of cliques Q , for different values of the density of inter-clique links γ . The bold segment, with slope 0.55, signals the transition between two different behaviors for large Q . For smaller and large γ , $\langle n_R \rangle$ approaches zero and a positive constant, respectively.

approach a constant value for large γ , while it decays to zero for small γ . The two regimes are separated by a zone where, in accordance with Eq. (10), $\langle n_R \rangle$ displays a power-law decay, as demonstrated by the bold straight line. From these results, the critical point γ_c turns out to be bound to the interval (0.69, 0.71). Additionally, a least-square linear fit in the log-log plot of the figure makes it possible to evaluate the power-law exponent as $\alpha\beta \approx 0.55$.

Once these estimates for γ_c and $\alpha\beta$ have been obtained, we go back to our numerical results for $\langle n_R \rangle$ as a function of γ for different values of Q , shown in Fig. 5. Equation (8) implies that, for an appropriate choice of the exponent β , they should collapse onto a single curve if $Q^{\alpha\beta} \langle n_R \rangle$ is plotted versus $Q^\beta |\gamma - \gamma_c|$. The resulting curve is, precisely, the graph of the function F . Tuning parameters to obtain the best collapse makes it possible in turn to improve the estimations for the critical point γ_c and the decay exponent $\alpha\beta$.

The main panel of Fig. 7 shows the outcome of this procedure. Our final estimation for the critical point and the critical exponents was $\gamma_c = 0.71(1)$, $\alpha = 1.3(1)$, and $\beta = 0.42(4)$, respectively. Errors were evaluated from an appraisal of the collapse quality as the parameters were slightly varied around their optimal values. The same method was

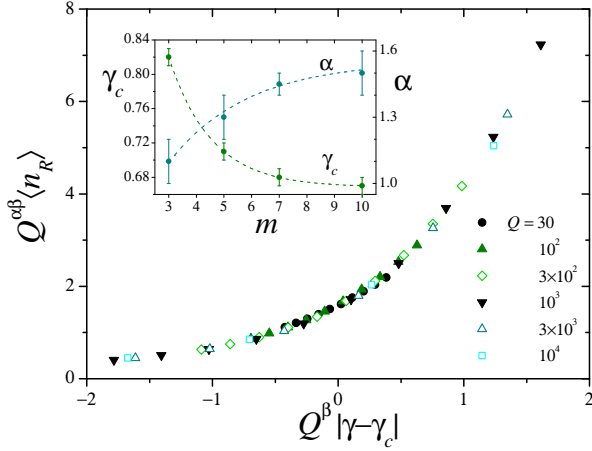


Figure 7: Main panel: Collapse of the data in the main panel of Fig. 5 over the plane spanned by the size-rescaled variables $Q^\beta |\gamma - \gamma_c|$ and $Q^{\alpha\beta} \langle n_R \rangle$, for $\gamma_c = 0.71$, $\alpha = 1.3$ and $\beta = 0.42$. Inset: Estimations for the critical point γ_c and the main critical exponent α as functions of the clique size m . Dashed curves show the results of least-square fittings with exponentially saturating functions for both datasets.

applied to another three values of the clique size m , obtaining the final results reported in Table 1. Within measurement uncertainties, the exponent β shows a negligible dependence on m . On the other hand, both γ_c and α exhibit a tendency to saturate as the clique size grows, as shown in the inset of Fig. 7. A phenomenological fitting of an exponential function of the form $y = y_0 + a \exp(-bx)$ yields, for the asymptotic values at large m , $\gamma_c^{\text{asympt}} = 0.67(1)$ and $\alpha^{\text{asympt}} = 1.55(5)$.

m	γ_c	α	β
3	0.82(1)	1.1(1)	0.42(4)
5	0.71(1)	1.3(1)	0.42(4)
7	0.68(1)	1.45(5)	0.39(3)
10	0.67(1)	1.5(1)	0.40(3)

Table 1: The critical value of the density of inter-clique links, γ_c , and the critical exponents α and β , obtained from finite-size scaling analysis for four values of the clique size m . The results for γ_c and α are plotted in the inset of Fig. 7.

V Conclusion

We have shown that a model process of rumor propagation between agents on a random network of cliques (RNoC) undergoes a critical transition induced by a change in the network structure. Specifically, as the density of inter-clique links increases and, hence, the network connectivity grows, the dynamics shift from a regime where the rumor remains confined to a negligible domain around its source to a regime where it spreads across a finite fraction of the population. The critical nature of the transition has been assessed by employing finite-size scaling analysis, which also made it possible to find the critical points and exponents. Both quantities depend on the size of individual cliques –and are thus not universal– approaching well-defined asymptotic values as the cliques become larger.

To keep the number of parameters in the problem at its minimum, we have considered random networks of cliques where all cliques have the same size. In the original formulation, however, these networks may be formed by cliques of different sizes, drawn at random from a prescribed distribution [18]. We have performed several series of simulations, not presented here, to verify that qualitatively the same behavior is obtained when clique sizes are distributed. With exponentially decaying distributions for clique sizes larger than or equal to three, the presence of large cliques implies a decrease in the effectiveness of propagation, much as that shown in Fig. 4, as the size grows sufficiently.

The critical phenomenon disclosed in this contribution is qualitatively the same as that which is found to occur in a similar model of rumor propagation on Watts-Strogatz small-world networks [15, 16]. In both models, the transition between rumor confinement and spreading is triggered by a growth in the degree of disorder of the underlying contact pattern. While in RNoCs disorder grows with the density of inter-clique connections γ , in small-world networks disorder is determined by the density of shortcuts (usually denoted as p [17]) between otherwise distant zones of the network. Because of their different meaning, a quantitative comparison between the critical values of γ and p is not possible. However, it is found in both cases that the transition threshold decreases when the average number of neighbors per node in-

creases (in the case of RNoCs, when m grows). On the other hand, the main critical exponent of the transition (α , in the present case) can be directly compared between the two models. It turns out that, in RNoCS, the critical exponent is smaller than in small-world networks, thus corresponding to a sharper growth of the order parameter just above the transition. Since the exponent is larger than one in both models, the two cases correspond to transitions where the first derivative of the order parameter with respect to the control parameter is continuous at the critical point.

The qualitative likeness between the critical phenomena found in RNoCs and small-world networks should be ascribed to some sort of underlying similarity between the two classes of contact patterns. As we have discussed in Section II, in fact, random networks of cliques do exhibit the structural properties that define small-world architectures, namely, large clustering induced by the high connectivity inside cliques, and short geodesic distances inherited from the random pattern of inter-clique connections. Such an analogy triggers the conjecture that the kind of critical transition observed in these models –and, probably, in a wider class of contact processes inspired by epidemiology and other transmission phenomena– may be systematically induced by the growth of disorder in the contact network, at an intermediate point along the resulting simultaneous decrease of clustering and geodesic distances. It remains to be verified whether other critical-like phenomena induced by disorder in small-world architectures –such as the onset of epidemiological oscillations in SIRS models [3]– also occur in populations interacting through random networks of cliques. The implications of these phenomena in more realistic settings are open to further research.

-
- [1] M E J Newman, A L Barabási, D J Watts, *The structure and dynamics of networks*, Princeton University Press, Princeton, NJ (2006).
- [2] M J Keeling, *The effects of local spatial structure on epidemiological invasions*, Proc. R. Soc. London B **266**, 859 (1999).
- [3] M N Kuperman, G Abramson, *Small world effect in an epidemiological model*, Phys. Rev. Lett. **86**, 2909 (2001).
- [4] R Pastor Satorras, C Castellano, P Van Mieghem, A Vespignani, *Epidemic processes in complex networks*, Rev. Mod. Phys. **87**, 925 (2014).
- [5] R Pastor Satorras, A Vespignani, *Epidemic spreading in scale-free networks*, Phys. Rev. Lett. **86**, 3200 (2001).
- [6] Yu Dan, Yang Jun-Zhong, *Effects of correlation between network structure and dynamics of oscillators on synchronization transition in a Kuramoto model on scale-free networks*, Commun. Theor. Phys. **61**, 197 (2014).
- [7] Yang Liu, J Kurths, *Effects of network robustness on explosive synchronization*, Phys. Rev. E **100**, 012312 (2019).
- [8] J T Lizier, F Bauer, F M Atay, J Jost, *Analytic relationship of relative synchronizability to network structure and motifs*, Proc. Nat. Acad. Sci. USA **120**, e2303332120 (2023).
- [9] V Pernice, S Cardanobile, S Rotter, *How structure determines correlations in neuronal networks*, PloS Comput. Biol. **7**, e1002059 (2011).
- [10] I Vlachos, A Aertsen, A Kumar, *Beyond statistical significance: Implications of network structure on neuronal activity*, PloS Comput. Biol. **8**, e1002311 (2012).
- [11] D Q Nykamp, D Friedman, S Shaker, M Shinn, M Vella, A Compte, A Roxin, *Mean-field equations for neuronal networks with arbitrary degree distributions*, Phys. Rev. E **95**, 042323 (2017).
- [12] M Pascual, J A Dunne, *Ecological networks: Linking structure to dynamics in food webs*, Oxford University Press, Oxford, UK (2006).
- [13] Guang-Zhong Wang, M J Lercher, *The effects of network neighbours on protein evolution*, PloS ONE **6**, e18288 (2011).
- [14] Y Guo, A Amir, *Exploring the effect of network topology, mRNA and protein dynamics on gene regulatory network stability*, Nat. Comm. **12**, 130 (2021).

- [15] D H Zanette, *Critical behavior of propagation on small-world networks*, *Phys. Rev. E* **64**, 050901(R) (2001).
- [16] D H Zanette, *Dynamics of rumor propagation on small-world networks*, *Phys. Rev. E* **65**, 041908 (2002).
- [17] D J Watts, S H Strogatz, *Collective dynamics of 'small-world' networks*, *Nature* **393**, 440 (1998).
- [18] L A Sobehart, S Martínez Alcalá, A Chacoma, D H Zanette, *Structural properties of random networks of cliques*, *Physica A* **624**, 128998 (2023).
- [19] M E J Newman, *The structure of scientific collaboration networks*, *Proc. Nat. Acad. Sci. USA* **98**, 404 (2001).
- [20] J Moody, D R White, *Structural cohesion and embeddedness: A hierarchical concept of social groups*, *Am. Sociol. Rev.* **68**, 103 (2003).
- [21] P Heady, *European kinship today: Patterns, prospects and explanations*, *Ethnol. Franc.* **42**, 93 (2012).
- [22] E Giuliani, *Clusters, networks and firms' product success: An empirical study*, *Manag. Decis.* **51**, 1135 (2013).
- [23] M Lawicka, *Clusters as networking organizations supporting the digital development of companies*, *Procedia Comput. Sci.* **207**, 3183 (2022).
- [24] E Ravasz, A L Somera, D A Mongru, Z N Oltvai, A L Barabási, *Hierarchical organization of modularity in metabolic networks*, *Science* **297**, 1551 (2002).
- [25] J A Dunne, R J Williams, N D Martínez, *Food-web structure and network theory: The role of connectance and size*, *Proc. Nat. Acad. Sci. USA* **99**, 12917 (2002).
- [26] T J Akiki, C G Abdallah, *Determining the hierarchical architecture of the human brain using subject-level clustering of functional networks*, *Sci. Rep.* **9**, 19290 (2019).
- [27] M Herzinger, S Lawrence, *Extracting knowledge from the world wide web*, *Proc. Nat. Acad. Sci. USA* **101**, 5186 (2004).
- [28] D J Watts, *Small worlds: The dynamics of networks between order and randomness*, Princeton University Press, Princeton, NJ (2004).
- [29] M Newman, *Networks. An introduction*, Oxford University Press, Oxford, UK (2010).
- [30] M E J Newman, S H Strogatz, D J Watts, *Random graphs with arbitrary degree distributions and their applications*, *Phys. Rev. E* **64**, 026118 (2001).
- [31] Zhenhua Yu, Si Lu, Dan Wang, Zhiwu Li, *Modeling and analysis of rumor propagation in social networks*, *Inform. Sci.* **580**, 857 (2021).
- [32] D Daley, D G Kendall, *Stochastic rumors*, *Math. Mod. Appl.* **1**, 42 (1965).
- [33] D P Maki and M Thompson, *Mathematical models and applications*, Prentice-Hall, Hoboken, NJ (1973).
- [34] A Sudbury, *The proportion of the population never hearing a rumour*, *J. Appl. Probab.* **22**, 443 (1985).
- [35] W E Schiesser, *A mathematical modeling approach to infectious diseases*, World Scientific, Singapore (2018).
- [36] D P Landau, K Binder, *A guide to Monte Carlo simulations in Statistical Physics*, Cambridge University Press, Cambridge, UK (2000).